

SPECTROSCOPIC STUDY OF THE CfA SAMPLE OF SEYFERT GALAXIES¹

DONALD E. OSTERBROCK AND ANDRÉ MARTEL

University of California Observatories, Board of Studies in Astronomy and Astrophysics, University of California, Santa Cruz, CA 95064

Received 1992 October 9; accepted 1993 March 18

ABSTRACT

High signal-to-noise ratio spectra were obtained of nearly all the Seyfert 2 galaxies in the CfA complete sample published by Huchra & Burg, and of some of the Seyfert 1's as well. Several of the Seyfert 2 galaxies have weak, broad components to their H α emission lines, and in some cases to H β as well, and thus are Seyfert 1.8 or 1.9 objects on the Lick Observatory classification system. Luminosity functions and mean absolute magnitudes were calculated separately for each type and for various groupings of the types. Our spectra confirm Huchra & Burg's conclusion that the CfA sample contains a higher fraction of Seyfert 1's than the Wasilewski sample, which therefore appears to be deficient in faint, reddened Seyfert 1 galaxies. Specific geometrical models and evolutionary pictures of AGNs are discussed.

All the Seyfert 1.8, 1.9, and 2 galaxy spectra were measured spectrophotometrically, and all, when plotted in diagnostic diagrams, lie in the AGN regions except for two objects barely outside the region on one diagram. These good signal-to-noise ratio spectra confirm that, as suspected earlier, many Seyfert 1.8, 1.9, and 2 galaxies have weak [Fe x] λ 6735 emission in their spectra. The broad components of the Seyfert 1.8 and 1.9 galaxies have large H α /H β intensity ratios, extending previous similar results.

Subject headings: galaxies: Seyfert — surveys

1. INTRODUCTION

Statistical studies of Seyfert galaxies are useful in trying to understand their physical nature, particularly in obtaining their luminosity function(s), and the relative numbers of various types of Seyfert galaxies. For such studies, a complete sample, known not to omit any Seyfert galaxies down to a particular apparent magnitude, is required. There are great difficulties in obtaining such a complete sample from an objective-prism or color survey, for although these methods are highly efficient in finding some types of Seyfert galaxies, each of them is biased against certain other types (see, e.g., Osterbrock 1987). The only way to be sure of having a complete sample is to take individual slit spectra of all galaxies down to the desired apparent magnitude limit. Since only roughly 1% of field galaxies down to a given apparent magnitude are Seyfert galaxies, it is a formidable task to obtain a reasonably large sample in this way.

However, the CfA Redshift Survey (Huchra et al. 1983) does provide such a sample complete down to $m_{z,w} \leq 14.5$ over a large fraction of the sky, defined by the limits

$$\delta \geq 0^\circ \text{ and } b \geq 40^\circ$$

or

$$\delta \geq -2.5^\circ \text{ and } b \leq -30^\circ.$$

Slit spectra were obtained of all 2399 galaxies fulfilling these criteria, and a list of all the Seyfert galaxies included among them was published by Huchra & Burg (1992, hereafter HB). A preliminary version of this list was published by Huchra, Wyatt & Davis (1982), and a somewhat later version by Edelson (1987). The final list is apparently essentially complete; HB state that in their CfA sample they found *all* AGNs (within the stated magnitude and position limits) discovered in other surveys.

In their paper HB classified the Seyfert galaxies into only the two types Seyfert 1 and Seyfert 2. For the necessarily relatively low signal-to-noise ratio spectra taken for a mass radial velocity survey, this is all that can be done, but a finer division into Seyfert 1, 1.5, 1.8, 1.9, and 2 is possible with better signal-to-noise (S/N) ratio data (Osterbrock 1987). The weak, broad components of the H I emission lines which characterize Seyfert 1.8 (H α and H β) and Seyfert 1.9 (H α only) spectra, in particular, are easily lost on less favorable S/N ratio spectral scans (Osterbrock 1981). Many of the Seyfert 1.8 and 1.9 galaxies appear as Seyfert 2's on such noisier scans (Osterbrock & Shaw 1988). But the more finely divided types appear to have real physical significance and may contain clues on the nature, structure, and evolution of AGNs (Goodrich 1989, 1990).

Hence our aim was to obtain good S/N ratio spectra of all the Seyfert galaxies in the HB CfA sample which are not clearly Seyfert 1 or 1.5, to classify them on the finer division system named above, to measure spectrophotometrically in the Seyfert 1.8, 1.9, and 2 spectra the various emission lines (including the broad and narrow components of the H I lines), to use these data to derive the luminosity functions of the various subtypes of Seyfert galaxies, and to discuss the results from the points of view of a unified model of AGNs and of an evolutionary picture.

2. OBSERVATIONS

Spectra were obtained with the CCD lens-grism spectrograph on the Shane 3 m reflector of Lick Observatory (Miller, Robinson, & Goodrich 1988). All the galaxies listed as Seyfert 2 in the CfA sample as published by Edelson (1987) were observed. As he states, the types given in his paper represent the then unpublished classifications of HB. We did not have their complete sample until it was published in 1992. We did not take spectra of most of the objects HB classified as Seyfert 1, because they are almost certain to be either Seyfert 1 or 1.5 on the Lick classification, and in fact for nearly all of them,

¹ UCO/Lick Observatory Bulletin, No. 1251.

preexisting Lick spectra, as well as the few we took in the current program, confirmed this. Our aim was to look for weak, previously unrecognized broad H α and H β emission-line components in the so-called Seyfert 2 galaxies' spectra. We did not take spectra of any of the galaxies classified by HB as LINERs, BL Lacertae objects, or weak-lined X-ray sources, nor of the quasar 3C 273, which they list as a Seyfert 1 object but discuss separately. All our spectra were taken with a TI 800 \times 800 CCD detector, and a long slit, 2" wide, centered on the nucleus. For each HB Seyfert 2 galaxy, we first obtained a good spectrum with a 420 lines mm⁻¹ grating, covering the range $\lambda\lambda$ 4000–8000 at a scale of 5.0 Å pixel⁻¹, giving a resolution of approximately 12 Å (FWHM). If the spectrum showed any sign of broad wings on H α or H β , we subsequently tried to obtain a good spectrum with a higher dispersion, 600 lines mm⁻¹ grating, covering the range $\lambda\lambda$ 4500–7200 at a scale of 3.6 Å pixel⁻¹ giving a resolution of approximately 8 Å.

We also obtained, with the same instrumental setups, spectra of several "normal" spiral and elliptical galaxies, to be used as template spectra in removing the integrated stellar absorption-line component of the Seyfert galaxy spectra, as described below. We tried to choose, to the extent possible, S0 or SB spirals, with relatively bright nuclei, in an effort to use galaxies as closely similar to the Seyfert galaxies as we could. The problem is that nearly all "normal" spirals have H α , H β , [N II], and [S II] emission lines in their spectra, at some level of strength, and we ended using the "continuum removal sources" with the weakest emission lines among the objects we had taken. Table 1 gives a journal of the low-dispersion observations, and Table 2, of the high-dispersion ones. The names used for the Seyfert galaxies are the same as those used by HB. Note that HB inadvertently omitted Mrk 471 from their Table 1, but included it in their statistical discussion and luminosity functions.

All the data were reduced following standard Lick Observatory procedures for bias subtraction, flat-field correction, wavelength calibration, flat-field correction, and flux calibration, as described, for instance, by Tran, Osterbrock, & Martel (1992).

3. CLASSIFICATION

All our spectra were classified Seyfert 1, 1.5, 1.8, 1.9, or 2 on the system described by Osterbrock (1987). These types are listed in Table 3. For the objects which we did not newly observe, types assigned by Dahari & De Robertis (1988, hereafter DD), based on earlier Lick spectra, or from other previously published or unpublished Lick classifications, including Goodrich (1989), are listed. Although the weak, broad components of H α and H β are sometimes difficult to see, we found that our classification agrees in most cases with the classification of these authors. Furthermore, independent classifications of different spectra of the same object gave the same types. The table then gives the consensus Lick type used in the rest of this paper, and the type given by HB. Both NGC 7603, also known as Mrk 530 (Tohline & Osterbrock 1976; Goodrich 1989), and Mrk 993 (Tran et al. 1992) have been observed to vary over the range from Seyfert 1 to 1.9 during the past 15 and 10 years, respectively; we adopt Seyfert 1.5 as the median or intermediate type of each. Likewise, NGC 4151 has been observed to have variable H I profiles over the past 20 years, being observed mostly as Seyfert 1.5, but occasionally as a Seyfert 1.8 or 1.9 (Cohen & Antonucci 1983; Penston &

TABLE 1
JOURNAL OF OBSERVATIONS: LOW DISPERSION

Object	UT Date	Exposure (minutes)
Mrk 334	1991 Sep 17	10
Mrk 335	1991 Sep 17	5
A0048+29	1991 Sep 17	15
Mrk 993	1991 Feb 6	25
	1991 Sep 17	20
	1991 Dec 12	30
Mrk 573	1991 Sep 17	5
0152+06	1991 Feb 6	30
NGC 863	1991 Sep 17	5
NGC 1144	1991 Sep 17	10
	1991 Sep 17	20
	1991 Sep 17	20
NGC 3079	1991 Feb 6	30
NGC 3362	1991 Feb 6	30
A1058+45	1991 Feb 6	25
NGC 5033	1991 Jun 7	5
1335+39	1991 Feb 6	20
NGC 5252	1991 Feb 6	30
NGC 5256 SW	1991 Jun 7	8
NGC 5256 NE	1991 Jun 7	8
NGC 5283	1991 Feb 6	25
NGC 5273	1991 Feb 6	30
NGC 5674	1991 Feb 6	25
NGC 5695	1991 Feb 6	25
NGC 5929	1991 May 7	20
NGC 5940	1991 Jun 7	10
NGC 6104	1991 May 7	30
2237+07	1991 Jun 7	5
NGC 7469	1991 Sep 17	5
Mrk 530	1991 Sep 17	8
NGC 7674	1991 Sep 17	8
NGC 7682	1991 Sep 17	10
	1991 Sep 17	10

TABLE 2
JOURNAL OF OBSERVATIONS: HIGH DISPERSION

Object	UT Date	Exposure (minutes)
Mrk 334	1991 Sep 18	10
	1991 Sep 18	15
Mrk 993	1991 Sep 18	30
Mrk 573	1991 Sep 18	10
	1991 Sep 18	10
0152+06	1991 Dec 12	30
	1991 Dec 12	45
NGC 1068	1991 Dec 12	0.3
	1991 Dec 12	0.3
NGC 1144	1991 Sep 18	40
1335+39	1991 Jun 8	20
	1991 Jun 8	25
NGC 5252	1991 May 8	60
NGC 5273	1991 Jun 8	15
	1991 Jun 8	25
NGC 5674	1991 Jun 8	25
NGC 7674	1991 Sep 18	15
	1991 Sep 18	15
NGC 7682	1991 Sep 18	25
	1991 Sep 18	25
M31	1991 Sep 18	3
	1991 Sep 18	3
M32	1991 Sep 18	1
	1991 Sep 18	1.5
	1991 Sep 18	1.5
NGC 1143	1991 Sep 18	40
NGC 6702	1991 Jun 7	20
	1991 Jun 8	30

Perez 1984). It is also listed as a Seyfert 1.5 in Table 3. HB classified Mrk 789 as a Seyfert 1, but we do not have a spectrum of it, as it was not included in the earlier list published by Edelson (1987). However, both DD and Véron-Cetty & Véron (1986) have classified it as a starburst (SB) or H II region galaxy, and we adopt that classification and omit it from our luminosity functions. In the further discussion, the consensus Lick Observatory types in the fifth column of Table 3 are used, except for the four objects not observed in that system, for

TABLE 3
SEYFERT GALAXY SPECTRAL TYPES

GALAXY	SEYFERT TYPE				
	This Paper	DD (1988)	Other LO	Consensus LO	HB (1992)
Mrk 334	1.8	1.8	...	1.8	2
Mrk 335	1	1	1	1	1
A0048+29	1	1	1
IZw 1	1	1.5	...	1	1
Mrk 993	1.5 ^a	2	...	1.5*	2
Mrk 573	2	2	...	2	2
0152+06	1.9	1.9	2
NGC 863	1	1.5	1.5	1	1
NGC 1068	2	2	2	2	2
NGC 1144	2	2	...	2	2
NGC 3080	...	1	1	1	1
NGC 3227	...	1.5	1.5	1.5	2
NGC 3362	2	2	2
A1058+45	2	2	2
NGC 3516	...	1.5	1.5	1.5	1
NGC 3786	...	1.8	1.8	1.8	1
NGC 3982	2
NGC 4051	...	1	1	1	1
NGC 4151	...	1.5	1.5	1.5	1
NGC 4235	...	1.5	1	1	1
NGC 4253	...	1.5	1.5	1.5	1
Mrk 205	...	1	1	1	1
NGC 4388	...	2	2	2	2
NGC 4395	1
Mrk 231	...	1	1	1	1
NGC 5033	1.9	1.9	...	1.9	1
Mrk 789	...	SB	...	SB	1
1335+39	1.8	1.8	2
NGC 5252	1.9	1.9	2
NGC 5256	2	2	...	2	2
NGC 5283	2	2	...	2	2
NGC 5273	1.9	1	...	1.9	1
Mrk 461	2
NGC 5347	2
Mrk 279	...	1.5	1	1	1
NGC 5548	...	1.5	1.5	1.5	1
Mrk 471	...	1.8	...	1.8	2
NGC 5674	1.9	1.9	2
Mrk 817	...	1.5	1.5	1.5	1
NGC 5695	2	2	...	2	2
Mrk 841	...	1.5	...	1.5	1
NGC 5929	2	2	...	2	2
NGC 5940	1	1	1
NGC 6104	1.5	1.5	1
2237+07	1.8	1.8	1
NGC 7469	1	1.5	1	1	1
Mrk 530	...	1.5	1.5 ^a	1.5	1
NGC 7674	2	2	...	2	2
NGC 7682	2	2	2

^a Adopted "median" or intermediate type; see text.

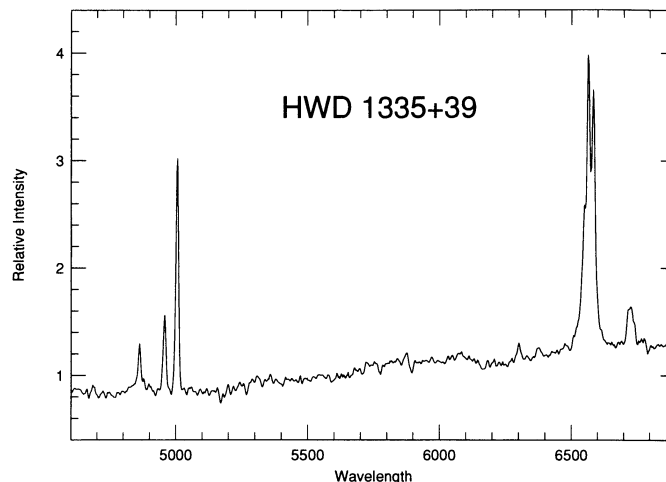


FIG. 1.—High-dispersion spectrum of HWD 1335+39, a Seyfert 1.8 galaxy

which the HB types in the sixth column are used. Spectra of HWD 1335+39, a Seyfert 1.8, and HWD 0152+06, a Seyfert 1.9, are shown in Figures 1 and 2, respectively, as samples of those types.

We found only a few large differences between our types and those of HB. Most of the objects which they classified Seyfert 1 are 1 or 1.5 on the Lick system, and most which they classified Seyfert 2 are 1.8, 1.9 or 2 on that system. However, there are a few exceptions.

It is interesting to compare the distribution of types in the CfA sample with those in the Wasilewski (1983) sample (Osterbrock & Shaw 1988), which is supposed to be complete to about $B = 15.5$. In the Wasilewski sample the numbers in types 1:1.5:1.8:1.9:2 are 2:2:1:1:9 for a total of 15 Seyfert galaxies. In the CfA sample the numbers, in the same order, are 13:10:4:6:15 for a total of 48 objects. These are very different distributions. According to the χ^2 test, there is only an 8% probability that these two samples are drawn from the same distribution. That they are drawn from different distributions can be seen even more easily if they are compressed into three groups, namely Seyfert 1+1.5, Seyfert 1.8+1.9, and Seyfert 2. For these three groups the relative numbers in the CfA sample

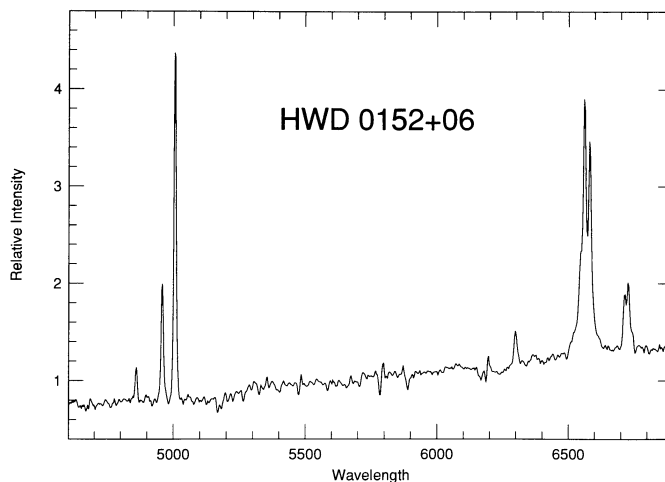


FIG. 2.—High-dispersion spectrum of HWD 0152+06, a Seyfert 1.9 galaxy

are 23:10:15, while in the Wasilewski sample they are 4:2:9. These are different distributions at the 2% significance level. Finally, in the most basic division Seyfert 1 + 1.5, and Seyfert 1.8 + 1.9 + 2, the relative numbers in the CfA sample are 23:25, while in the Wasilewski sample they are 4:11. These differ at the 3% significance level. Evidently the CfA sample is considerably richer in the strong broad-line types, and the Wasilewski sample is richer in the strong narrow-line types. HB found this result with their types, namely 26 Seyfert 1 and 23 Seyfert 2 galaxies (as stated in the text of their paper), omitting 3C 273 from the count of Seyfert 1's (though it is listed as one in their Table 1), and including Mrk 471 as a Seyfert 2 (though it was inadvertently omitted from the table).

The difference between these two samples is much too large to be accounted for by pure chance. The CfA sample should definitely be complete, from the way it was taken. This suggests that the Wasilewski sample is incomplete in the sense that some Seyfert 1 (and 1.5) galaxies are omitted from it. HB suggest that this occurred because Wasilewski's objective-prism search was more sensitive to the narrow emission lines of the Seyfert 2's, but missed a sensible fraction of the Seyfert 1's. However, the Wasilewski area is included in the region surveyed by Markarian and his collaborators with a lower dispersion objective prism, seeking ultraviolet-excess objects, which previous evidence seemed to show *had* identified most Seyfert 1 galaxies down to $B \approx 15.5$ (Lipovetsky, Markarian, & Stepanian 1987; Salzer 1989). This discrepancy points up the need for a concerted search for faint, reddened Seyfert 1 and 1.5 galaxies (or actually, any type of fainter Seyfert galaxies) in the Wasilewski area. In fact, Bothun et al. (1989) have already found, among the Wasilewski galaxies, one additional Seyfert 1 and three Seyfert 2's, two of them members of a close pair with ~ 10 kpc separation. Unless such a search turns up appreciably more Seyfert 1's with $B \leq 15.5$, the conclusion would have to be that the statistics of Seyfert galaxies are different in these two regions, one covering an appreciable fraction of the northern sky, the other, a smaller area near the north Galactic pole with magnitude limit only one magnitude fainter. This is perhaps not unexpected, for in these magnitude-limited samples, the more luminous Seyfert 1 galaxies are on the average at larger distances than the Seyfert 2 galaxies, and hence density inhomogeneities (such as the local supercluster and the "Great Wall") can affect the relative numbers of these objects.

The CfA sample should be essentially complete, and in addition it contains over 3 times as many objects as the Wasilewski sample. Hence, the CfA sample appears to be the one to use in discussing the luminosity function and space densities of Seyfert galaxies.

4. EMISSION-LINE FLUXES

The main purpose for which the spectra were taken was to make spectrophotometric measurements of the relative intensities of the individual emission lines. These were carried out using the Lick VISTA software package. For each Seyfert 1.8, 1.9, or 2 galaxy, the observed spectrum of the nucleus was measured, summing over the pixels (typically 8) covering the brightest region (typically $5''$) along the center of the slit. Many absorption lines and features of the integrated stellar spectrum are seen in many of these spectra. To measure the weaker emission lines and the weak broad emission components as accurately as possible, an attempt was made to remove the

absorption lines by subtracting a scaled spectrum of a "normal" galaxy (see, e.g., Filippenko 1985). This was done by assuming the observed Seyfert galaxy spectrum, F_λ , to be the sum of three components: a pure emission-line component; a "featureless continuum" represented by a quadratic in wavelength, $A\lambda^2 + B\lambda + C$; and an observed "template-galaxy" spectrum $DF_\lambda(G)$. The template-galaxy spectrum was broadened, if necessary, so that the width of its absorption lines best matched the widths of the absorption lines in the Seyfert galaxy spectrum, and A , B , C and D were varied to give the best overall fit, excluding all the emission lines. If the Seyfert galaxy spectrum had narrower lines, it was broadened so that its absorption lines best matched those in the template galaxy spectrum, and the constants were similarly varied to give the best fit. Then, keeping the values of A , B , C , and D fixed, the *unbroadened* Seyfert galaxy spectrum was used in the subtraction. This gives the best overall fit to the line fluxes, without degrading the observed spectrum of the Seyfert galaxy. The final subtraction is a bit noisier in such cases, but the Seyfert galaxy spectrum has not suffered any less in resolution. Various template galaxies were tried, and the best subtraction was used. The spectrum of an example, NGC 5273 as observed, and the same spectrum after subtraction of the featureless continuum and the M32 template spectrum, are shown in Figure 3. Note that we classified it as a Seyfert 1.9 (no broad $H\beta$ emission component visible) on the basis of the observed spectrum, but after the subtraction the broad $H\beta$ feature, though very weak, became visually detectable.

The emission-line fluxes were then measured on the subtracted spectra (if available) of all the Seyfert 1.8, 1.9, and 2 galaxies. All the easily seen narrow lines were measured, as well as the broad components of $H\alpha$ and $H\beta$. Although we had attempted to avoid saturating the CCD in any of the lines when taking the spectra, we often worked close to the limit in order to get good S/N ratio data for the integrated stellar absorption-line spectrum and the fainter lines. With an accurately determined value of the count at saturation, it turned out later than in a very few of the spectra a few pixels in [O III]

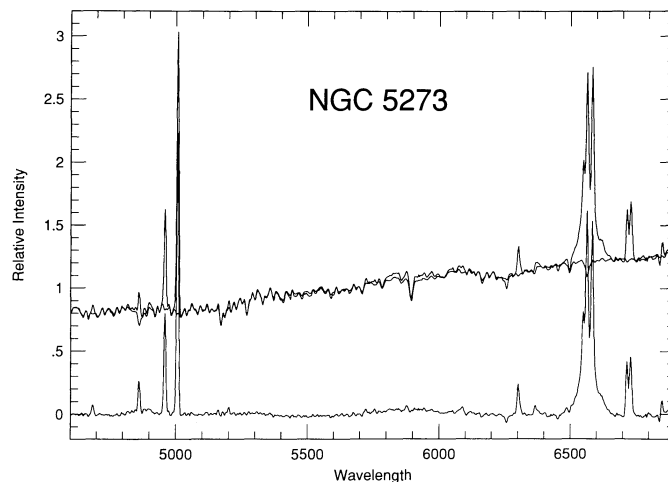


FIG. 3.—High-dispersion spectrum of NGC 5273, a Seyfert 1.9 galaxy. Upper, as observed, and, nearly coincident with it except in the emission lines, scaled template spectrum of M32; lower is difference, almost pure emission-line spectrum of NGC 5273. Both are plotted with same intensity scale and zero point.

$\lambda 5007$ or the narrow component of $H\alpha$ ($H\alpha_n$ hereafter) were saturated. However, in none of these cases did the measured value of the $[\text{O III}]\lambda 5007/\lambda 4959$ differ significantly from the calculated value 2.88. Hence the effect of the few saturated pixels on the total line fluxes was minimal, and the measurements were used if no other, unsaturated ones were available.

The lines were measured individually, except that the $H\alpha_n$, $[\text{N II}]\lambda\lambda 6548, 6583$ blend, the $[\text{S II}]\lambda\lambda 6716, 6731$ blend (abbreviated $\lambda 6724$), and the $[\text{O I}]\lambda 6364, [\text{Fe X}]\lambda 6375$ blend (abbreviated $\lambda 6364$, its usual peak wavelength) were measured as units, and then deblended. In deblending the $H\alpha$, $[\text{N II}]$ complex the intensity ratio $[\text{N II}]\lambda 6583/\lambda 6548 = 2.94$ (from the calculated transition probabilities and known wavelengths) was used as a known constant, and the intensity ratios of $H\alpha_n/[\text{N II}]\lambda 6583$, and of $r = [\text{S II}]\lambda 6716/\lambda 6731$ were varied to get the best overall fit.

The flux in $[\text{O I}]\lambda 6364$ was calculated from the known intensity $[\text{O I}]\lambda 6300/\lambda 6364 = 3.04$, and then the flux in $[\text{Fe X}]\lambda 6375$ was calculated by subtraction from the flux in the $\lambda 6364$ blend. All the fluxes were measured in relative units, normalized to $[\text{O III}]\lambda 4959$. These relative fluxes, for the stronger narrow lines used in the three diagnostic ratios recommended by Veilleux & Osterbrock (1987), measured on the high-dispersion spectra, are listed in Table 4, and measured on the low-dispersion spectra, in Table 6. Note that these relative fluxes are given in logarithmic form, except for $r = [\text{S II}]\lambda 6716/\lambda 6731$ in the last column. The measurements of the other, weaker narrow lines are listed in Tables 5 and 7. In each table the upper line for each object gives its measured, relative

fluxes; the lower lines gives these same fluxes, corrected for interstellar extinction, as discussed below.

All the measured narrow-line fluxes were then corrected for interstellar extinction, using the method discussed, for instance, by Veilleux & Osterbrock (1987). The intrinsic ratio in AGNs was taken to be $I(H\alpha)/I(H\beta) = 3.1$, and the Whitford reddening curve was used. The numerical value of the derived reddening constant c is listed in the lower row for each object, in the right-hand column of Tables 4 and 6. Note for two objects, NGC 5283 and NGC 5695, the observed ratio of fluxes $F(H\alpha)/F(H\beta)$ was close to but smaller than 3.1, indicating observational error or that the actual intrinsic ratio is less than this value in these two objects. For them the reddening was taken to be zero ($c = 0$).

The weak, broad components of $H\alpha$ and $H\beta$ were also measured in the Seyfert 1.8 and 1.9 galaxies. These broad lines are considerably more difficult to define accurately than the narrow lines, and placement of the continuum is crucial. The broad-line fluxes relative to $[\text{O III}]\lambda 4959$ are listed in the second and fourth columns of Table 8 for each object. As before, the first entry is the measured quantity, while the second entry is that same quantity corrected for interstellar extinction. The ratio of the two broad lines is given in the sixth column. The reddening correction for the broad lines were based on the values of c derived from the narrow lines. The interpretation of these data is discussed below, in § 6.

5. LUMINOSITY FUNCTION

One of the main aims of our program was to derive luminosity functions for the various types of Seyfert galaxies in the

TABLE 4
LOGARITHMS OF MEASURED AND CORRECTED EMISSION-LINE RATIOS:^a HIGH-DISPERSION DATA

Object	$H\beta_n$	$[\text{O III}]\lambda 5007$	$[\text{O I}]\lambda 6300$	$[\text{N II}]\lambda 6548$	$H\alpha_n$	$[\text{N II}]\lambda 6583$	$[\text{S II}]\lambda 6724$	r c
Mrk 334	0.27	0.54	-0.25	0.36	1.06	0.83	0.53	1.14
	0.30	0.53	-0.49	0.09	0.79	0.56	0.24	0.89
Mrk 993	-0.46	0.48	-0.30	0.12	0.29	0.59	0.25	1.03
	-0.44	0.48	-0.50	-0.11	0.06	0.36	0.00	0.75
Mrk 573	-0.58	0.43	-0.96	-0.55	0.01	-0.10	-0.28	1.07
	-0.58	0.43	-1.04	-0.64	-0.08	-0.19	-0.37	0.29
0152+06	-0.47	0.48	-0.38	-0.31	0.29	0.16	-0.01	0.94
	-0.45	0.47	-0.59	-0.56	0.05	-0.09	-0.28	0.81
NGC 1068	-0.58	0.47	-0.85	-0.44	...

NGC 1144	-0.42	0.46	-0.49	-0.05	0.14	0.42	0.07	...
	-0.42	0.46	-0.55	-0.12	0.08	0.35	0.00	0.21
1335+39	-0.25	0.47	-0.62	-0.02	0.47	0.45	-0.09	1.20
	-0.24	0.47	-0.80	-0.22	0.27	0.24	-0.31	0.65
NGC 5252	-0.38	0.47	-0.19	-0.35	0.19	0.12	0.10	1.13
	-0.37	0.47	-0.25	-0.41	0.12	0.06	0.03	0.22
NGC 5273	-0.52	0.46	-0.44	-0.27	0.21	0.20	0.01	0.94
	-0.50	0.45	-0.64	-0.49	-0.01	-0.02	-0.23	0.72
NGC 5674	-0.38	0.43	-0.49	-0.21	0.31	0.25	0.06	1.26
	-0.36	0.42	-0.65	-0.40	0.13	0.07	-0.13	0.59
NGC 7674	0.57	0.46	-0.92	-0.47	0.09	0.01	-0.43	0.95
	-0.56	0.45	-1.05	-0.62	-0.06	-0.14	-0.59	0.48
NGC 7682	-0.52	0.46	-0.47	-0.32	0.13	0.14	-0.01	0.95
	-0.51	0.46	-0.59	-0.46	-0.01	0.00	-0.16	0.46

^a Normalized with respect to $[\text{O III}]\lambda 4959$.

TABLE 5
LOGARITHMS OF MEASURED AND CORRECTED EMISSION-LINE RATIOS:^a
HIGH-DISPERSION DATA

Object	He II λ4686	[N I] λ5199	[Fe VII] λ6087	Blend λ6364	[O I] λ6364	[Fe X] λ6375
Mrk 334	-0.70	...	-0.62	-0.73	-1.26
	...	-0.75	...	-0.87	-0.98	-1.50
Mrk 993	-0.85	-0.82	-0.55	-0.78	-0.94
	...	-0.90	-1.00	-0.76	-0.99	-1.15
Mrk 573	-1.02	-1.64	-1.22	-1.27	-1.44	-1.75
	-1.00	-1.66	-1.29	-1.35	-1.52	-1.83
0152+06	-0.85	-0.86	-2.79
	-1.08	-1.08	-3.02
NGC 1068	-1.10	-1.49	-1.28	-1.27	-1.34	-2.10

NGC 1144	-1.02	-1.00	...	-1.00	-0.98	...
	-1.01	-1.01	...	-1.06	-1.04	...
1335+39	-0.85	-1.10	...	-0.92	-1.10	-1.39
	-0.81	-1.14	...	-1.10	-1.28	-1.57
NGC 5252	-1.18	-1.14	...	-0.66	-0.68	-2.04
	-1.16	-1.16	...	-0.72	-0.74	-2.10
NGC 5273	-0.85	-1.17	-1.04	-0.82	-0.92	-1.50
	-0.80	-1.21	-1.21	-1.03	-1.13	-1.71
NGC 5674	-1.02	-1.08	-1.47	-0.96	-0.98	-2.34
	-0.97	-1.11	-1.61	-1.12	-1.14	-2.51
NGC 7674	-1.14	-1.68	-1.27	-1.40	-1.40	-3.34
	-1.11	-1.71	-1.38	-1.53	-1.54	-3.47
NGC 7682	-1.21	-1.22	...	-0.96	-0.95	...
	-1.17	-1.25	...	-1.09	-1.08	...

^a Normalized with respect to [O III]λ4959.

CfA sample. We wished to treat, in particular, the Seyfert 1.8 and 1.9 galaxies separately, and compare the results derived from the CfA sample with those derived earlier for the Wasilowski field by Osterbrock & Shaw (1988), and from the UM survey by Salzer (1989).

HB calculated the luminosity functions or space densities of all the Seyfert galaxies in the CfA sample, and of the Seyfert 1 and Seyfert 2 galaxies (according to their classification) separately. They used the V/V_m method, and we simply followed their procedures as closely as we could, to make the results as nearly comparable as possible. The basic idea of the method, as described by Schmidt (1968) and by Huchra & Sargent (1973), is to form the luminosity function as a sum

$$\phi(M) = \frac{4\pi}{\Omega} \sum_i \frac{1}{V_m^i}$$

over all the galaxies in the range of absolute magnitude between M and $M + \Delta M$, where V_m^i is the maximum spherical volume within which that galaxy would still fall in the sample (determined by the apparent magnitude limit of the sample), $\Omega/4\pi$ is the fraction of the sky covered by the sample, and ΔM is the interval of absolute magnitude binned together, 0.5 in this case. HB determined the distances from their measured radial velocities, corrected for a Virgocentric flow, assuming a Hubble constant $H_0 = 100 \text{ km s}^{-1} \text{ Mpc}^{-1}$. They very kindly sent us a list of the measured and corrected radial velocities, and of the derived distances and absolute magnitudes for all the galaxies, and allowed us to use it in this paper. They used $\Omega = 2.15 \text{ sr}$ for the area of the sky covered by the CfA survey, corresponding to the fractional area $\Omega/4\pi = 0.171$, and we follow them in this.

We then calculated the luminosity functions for all the Seyferts together (differing from HB only in excluding Mrk 789), for Seyfert 1, 1.5, 1.8, 1.9, and 2 separately, and for the galaxies grouped as Seyfert 1 and 1.5 together, 1.8 and 1.9 together, and

TABLE 6
LOGARITHMS OF MEASURED AND CORRECTED EMISSION-LINE RATIOS:^a LOW DISPERSION DATA

Object	Hβ(<i>n</i>)	[O III] λ5007	[O I] λ6300	[N II] λ6548	Hα(<i>n</i>)	[N II] λ6583	[S II] λ6724	<i>r</i> <i>c</i>
NGC 3362	-0.46	0.48	-0.55	0.02	0.11	0.48	0.05	...
	-0.45	0.47	-0.61	-0.05	0.04	0.42	-0.02	0.22
A1058+45	-0.70	0.46	-0.92	-0.43	-0.05	0.04	-0.40	...
	-0.69	0.45	-1.05	-0.58	-0.19	-0.11	-0.55	0.47
NGC 5033	-0.32	0.42	-0.16	0.47	0.50	0.94	0.40	...
	-0.29	0.41	-0.43	0.17	0.19	0.63	0.07	1.00
NGC 5256 SW	-0.14	0.46	-0.64	-0.08	0.69	0.39	0.27	...
	-0.12	0.45	-0.91	-0.40	0.37	0.07	-0.07	1.03
NGC 5256 NE	0.28	0.44	0.09	0.26	0.91	0.73	0.62	...
	0.29	0.44	-0.03	0.13	0.78	0.60	0.47	0.43
NGC 5283	-0.31	0.48	-0.44	-0.41	0.12	0.06	0.01	...
	-0.31	0.48	-0.44	-0.41	0.12	0.06	0.01	0.00
NGC 5695	-0.47	0.45	-0.70	-0.32	-0.01	0.15	-0.10	...
	-0.47	0.45	-0.70	-0.32	-0.01	0.15	-0.10	0.00
NGC 5929	-0.17	0.43	-0.06	-0.13	0.55	0.34	0.40	...
	-0.15	0.42	-0.24	-0.34	0.34	0.12	0.18	0.68
2237+07	-0.21	0.43	-0.77	-0.23	0.44	0.24	-0.55	...
	-0.20	0.42	-0.90	-0.38	0.29	0.09	-0.72	0.50

^a Normalized with respect to [O III]λ4959.

TABLE 7
LOGARITHMS OF MEASURED AND CORRECTED EMISSION-LINE RATIOS:^a
LOW-DISPERSION DATA

Object	He II λ4686	[N I] λ5199	[Fe VII] λ6087	Blend λ6364	[O I] λ6364	[Fe X] λ6375
NGC 3362	-1.16	...	-0.92	-1.04	-1.56
	...	-1.17	...	-0.98	-1.10	-1.62
A1058+45	-1.37	-1.40	-2.46
	-1.50	-1.53	-2.59
NGC 5033	-0.64	...
	-0.92	...
NGC 5256 SW	-0.85	-1.12	-1.19
	-1.14	-1.41	-1.48
NGC 5256 NE	-0.74	...	-0.34	-0.39	-1.26
	...	-0.77	...	-0.46	-0.51	-1.38
NGC 5283	-0.96	-0.92	...
	-0.96	-0.92	...
NGC 5695	-0.70	-1.18	-0.87
	-0.70	-1.18	-0.87
NGC 5929	-0.42	-0.54	-1.05
	-0.61	-0.73	-1.24
2237+07	-1.05	-1.25	-1.48
	-1.19	-1.39	-1.62

^a Normalized with respect to [O III]λ4959.

1.8, 1.9 and 2 together, which appear to be in some ways physically significant groups. The results are listed in Table 9. In each group the left-hand column gives the $\log \phi$, the logarithm of the luminosity function in galaxies $\text{Mpc}^{-3} \text{mag}^{-1}$, and the right-hand column gives the number of observed galaxies in the bin. At the bottom of each column the mean $\langle V/V_m \rangle$ for all the objects in the group is listed. For a homogeneous density distribution in Euclidean space, $\langle V/V_m \rangle = 0.50$, and deviations from this value are a good test of completeness or of one of the other assumptions stated (Schmidt 1968; Felten 1977).

The probable error of $\langle V/V_m \rangle$ as given by HB is $(12n)^{-1/2}$, where n is the total number of objects in the group. It is the

TABLE 8
MEASURED AND CORRECTED EMISSION-LINE RATIOS

Object	Hβb ^a	Hβn ^a	Hαb ^a	Hαn	$\frac{H\alpha b}{H\beta b}$	$\frac{H\alpha b}{H\alpha n}$
Mrk 334	0.59	1.88	3.72	11.56	6.3	0.3
	0.62	1.98	1.98	6.14	3.2	0.3
Mrk 993	0.59	0.35	5.60	1.96	9.5	2.9
	0.62	0.37	3.28	1.14	5.3	2.9
0152+06	0.19	0.34	2.06	1.97	10.8	1.0
	0.20	0.36	1.16	1.11	5.8	1.0
1335+39	0.80	0.56	3.00	2.97	3.8	1.0
	0.83	0.58	1.89	1.87	2.3	1.0
NGC 5273	0.30	0.30	3.28	1.62	10.9	2.0
	0.31	0.31	1.96	0.97	6.3	2.0
NGC 5033	2.30	0.48	6.86	3.17	3.0	2.2
	2.44	0.51	3.38	1.56	1.4	2.2
2237+07	0.28	0.61	2.13	2.78	7.6	0.8
	0.29	0.63	1.49	1.94	5.1	0.8

^a Normalized with respect to [O III]λ4959.

statistical uncertainty due to the finite number of objects. For comparison with HB we list it as the probable error in the next to last row for each of the groups in Table 9.

However, there is an additional source of error due to the uncertainties in the apparent magnitudes, $\delta m_b \approx 0.3$ mag rms according to HB. It is straightforward to show that the probable error in $\langle V/V_m \rangle$ due to these magnitude errors alone is

$$\frac{0.6 \ln 10}{n} \left[\sum_{i=1}^n \left(\frac{V}{V_m} \right)_i^2 \right]^{1/2} \delta m_b.$$

For the CfA Seyfert galaxy samples, this source of probable error is in fact comparable with that due to the finite number of objects in the group. The total error of $\langle V/V_m \rangle$ is the square root of the quadratic sum of these two separate errors, which for the CfA sample of Seyfert galaxies is thus approximately 1.2–1.5 times the error due to the finite number of objects in the group. We list this total, more nearly correct probable error in the last row of each of the groups in Table 9.

There is one object at considerably fainter absolute magnitude, NGC 4395, the “dwarf” Seyfert 1 galaxy studied by Filippenko & Sargent (1989), with $M_{Zw} = -16.3$. It is not included in any of the tabulated luminosity functions in HB or the present paper.

As we use five classification types for Seyfert galaxies, there are fewer objects in each type than in HB’s system of using only two types. Hence in our classification there is considerably more scatter in the luminosity functions of the individual types. On the other hand, putting Seyfert 1 and 1.5 together in one group, and Seyfert 1.8, 1.9, and 2 in another, our results are very similar to those of HB, for these are mostly their Seyfert 1’s and 2’s, respectively. Figure 4 shows a plot of the galaxies separated into three groups, Seyfert 1+1.5, Seyfert 1.8+1.9, and Seyfert 2. It emphasizes that at the highest luminosities essentially all Seyferts are Seyfert 1’s, while at the lowest luminosities shown on the group, most are Seyfert 1.8, 1.9, and 2. The number of Seyfert 1.8 and 1.9 galaxies per unit volume of space is significantly less than the number of Seyfert 2’s, although in some magnitude ranges this is not the case for the CfA sample, because of the statistics of small numbers.

This is emphasized in Figure 5, which shows the integral luminosity function of galaxies more luminous than a given

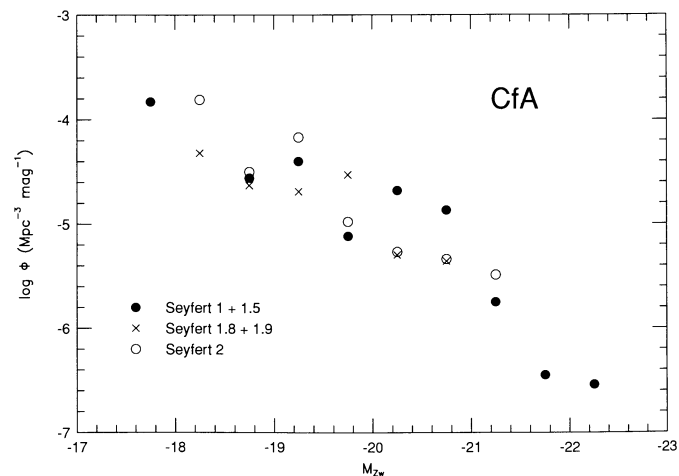


FIG. 4.—Luminosity functions of three groups of Seyfert-galaxy types, from CfA sample.

TABLE 9
LUMINOSITY FUNCTIONS

Bin	Seyfert 1		Seyfert 1.5		Seyfert 1.8		Seyfert 1.9		Seyfert 2		Seyfert 1 + 1.5		Seyfert 1.8 + 1.9		Seyfert 1.8 + 1.9 + 2		All Seyferts	
	log ϕ	n	log ϕ	n	log ϕ	n	log ϕ	n	log ϕ	n	log ϕ	n	log ϕ	n	log ϕ	n	log ϕ	n
-17.5 to -18.0	-3.83	1	...	0	...	0	...	0	...	0	-3.83	1	...	0	...	0	-3.83	1
-18.0 to -18.5	...	0	...	0	...	0	-4.32	1	...	3	...	0	-4.32	1	...	4	-3.69	4
-18.5 to -19.0	...	0	...	1	...	1	...	0	-4.50	1	-4.56	1	-4.62	1	-4.26	2	-4.08	3
-19.0 to -19.5	-4.84	1	-4.59	2	...	0	-4.69	1	-4.17	4	-4.40	3	-4.69	1	-4.06	5	-3.89	8
-19.5 to -20.0	...	0	-5.12	1	-4.82	2	-4.84	2	-4.98	1	-5.12	1	-4.53	4	-4.39	5	-4.32	6
-20.0 to -20.5	-4.89	4	-5.09	2	-5.30	1	...	0	-5.27	1	-4.68	6	-5.30	1	-4.99	2	-4.51	8
-20.5 to -21.0	-5.19	3	-5.15	3	...	0	-5.35	2	-5.34	2	-4.87	6	-5.35	2	-5.04	4	-4.65	10
-21.0 to -21.5	-6.10	1	-6.00	1	...	0	...	0	-5.48	3	-5.75	2	...	0	-5.48	3	-5.29	5
-21.5 to -22.0	-6.45	1	...	0	...	0	...	0	...	0	-6.45	1	...	0	...	0	-6.45	1
-22.0 to -22.5	-6.54	1	...	0	...	0	...	0	...	0	-6.54	1	...	0	...	0	-6.54	1
$\langle V/V_m \rangle$	0.61 \pm 0.08		0.38 \pm 0.09		0.64 \pm 0.14		0.57 \pm 0.12		0.41 \pm 0.07		0.51 \pm 0.06		0.60 \pm 0.09		0.48 \pm 0.06		0.49 \pm 0.04	
	0.61 \pm 0.12		0.38 \pm 0.11		0.64 \pm 0.20		0.57 \pm 0.17		0.41 \pm 0.09		0.51 \pm 0.08		0.60 \pm 0.13		0.48 \pm 0.08		0.49 \pm 0.06	

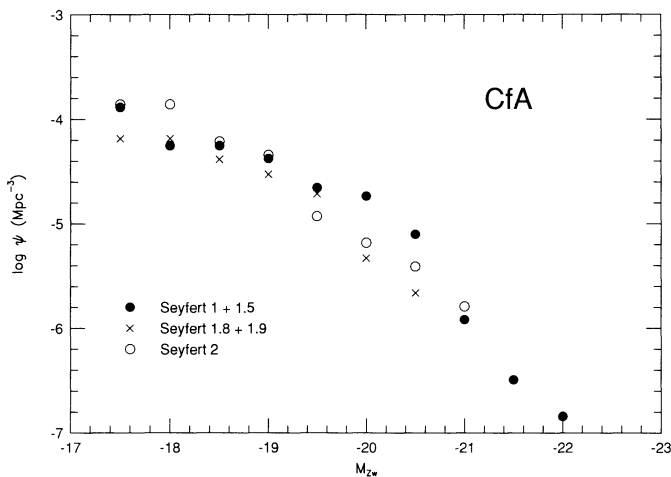


FIG. 5.—Integral luminosity function of galaxies more luminous than a given absolute magnitude, of three groups of Seyfert-galaxy types, and all Seyfert galaxies, from CfA sample.

absolute magnitude,

$$\psi(M_{Zw}) = \sum_{M'_{Zw}} \phi(M'_{Zw}) \Delta M'_{Zw}$$

for the various groupings separately. In this CfA sample all Seyfert galaxies more luminous than -21.5 are Seyfert 1's (as HB stated), down to about -19.5 , they are the most numerous of the three groups shown (down to about -20.0 if compared with the single group Seyfert 1.8+1.9+2 together), and the Seyfert 1.8+1.9 group is less numerous than the Seyfert 2's at nearly all absolute magnitudes.

Down to $M_{Zw} = -18.0$, the relative numbers of Seyfert 1+1.5 (per unit volume of space) to Seyfert 1.8+1.9 to Seyfert 2 is thus 0.22:0.25:0.53. This corresponds to a higher proportion of the first two groups than in the Wasilewski (1983) sample, which covers a smaller fraction of sky (0.25 sr) to a fainter apparent magnitude limit ($m_{Zw} \approx 15.5$). In it Osterbrock & Shaw (1988) found 0.12:0.10:0.78 for the same ratios. This discrepancy results directly from the different relative proportions of the various types of galaxies down to a given apparent magnitude mentioned in § 3.

The statistical uncertainties are difficult to assess, but one measure is the $\langle V/V_m \rangle$ test of Table 9. Each of the groups satisfies this test to within one standard deviation, except the Seyfert 1.5 galaxies, which fail by just 0.01. Note in particular that the Seyfert 1.8 and 1.9 galaxies do satisfy this test separately to within one standard deviation, which, however, is large because of the small number of objects in each group. It is clear that the classification of these objects with weak broad lines is close to the limit of our current observational methods, but is physically meaningful.

HB determined the relative space densities of Seyfert 2 to 1 galaxies in the CfA sample as 2.3 ± 0.7 , down to absolute magnitude $M_{Zw} = -18$. In our classification this corresponds to the ratio of space densities of Seyfert 1.8+1.9+2 to Seyfert 1+1.5, for which we find the value 3.6. The difference from HB's result is due to differences in classification of a few of the objects. Our spectra have much better signal-to-noise ratio than HB's, as they could only spend a small amount of observing time per object. The probable error of our result, just from the finite number of observed galaxies in each group, could be

TABLE 10
MEAN ABSOLUTE MAGNITUDES AND DISPERSIONS

Seyfert	$\langle M_{Zw} \rangle$	σ
1	-20.0	0.7
1.5	-19.4	0.7
1.8	-19.3	0.6
1.9	-18.9	0.7
2	-18.7	0.6
1 + 1.5	-19.6	0.7
1.8 + 1.9	-19.0	0.7
1.8 + 1.9 + 2	-18.8	0.7
All	-19.0	0.8

written 3.6 ± 1.0 . For the Wasilewski sample, this same ratio of space density of Seyfert 1.8+1.9 to 2 to Seyfert 1+1.5 is 7.3 (Osterbrock & Shaw 1988), while for the UM survey, roughly comparable to the Wasilewski sample in limiting magnitude but over a different region of the sky, Salzer (1989) found 5.3 ± 2.4 . As the discussion in § 5 above states, the Wasilewski survey evidently missed some Seyfert 1 and 1.5 galaxies; this was evidently less of a problem, but still present, in the UM survey.

The derived mean absolute magnitudes $\langle M_{Zw} \rangle$, and dispersions, σ , defined by

$$\langle M_{Zw} \rangle \sum_{M'_{Zw}} \phi(M'_{Zw}) \Delta M'_{Zw} = \sum M'_{Zw} \phi(M'_{Zw}) \Delta M'_{Zw}$$

$$\sigma^2 \sum \phi(M'_{Zw}) \Delta M'_{Zw} = \sum_{M'_{Zw}} (M'_{Zw} - \langle M_{Zw} \rangle)^2 \phi(M'_{Zw}) \Delta M'_{Zw}$$

for the CfA Seyferts, are listed in Table 10. (Note that, like HB, we have only extended these sums down to $M_{Zw} = -18$, because the last bin, -17.5 to -18.0 , may be seriously incomplete.) The tabulated absolute magnitudes show a clear progression with type. It has long been known that on average the Seyfert 1's are more luminous than Seyfert 2's, but this table provides a quantitative breakdown to the finer spectral subdivisions.

6. DISCUSSION

The CfA sample is presumably the most nearly representative known sample of Seyfert galaxies. Hence it is instructive to plot all the Seyfert 1.8, 1.9, and 2 galaxies in the diagnostic diagrams originated by Baldwin, Phillips & Terlevich (1981). Figures 6, 7, and 8 show the three ratios particularly recommended by Veilleux & Osterbrock (1987) for their relative insensitivity to errors in calibration over a wide wavelength interval, and to errors in reddening. It can be seen that all the observed points, except for two objects in the $[\text{O III}]/\text{H}\beta$ versus $[\text{S II}]/\text{H}\alpha$ diagram, fall in the AGN regions on these diagrams, to the right of the boundary lines found empirically by Veilleux & Osterbrock (1987).

Also, these good signal-to-noise ratio spectra seem to confirm what has been suspected several times earlier, namely that many Seyfert 1.8, 1.9, and 2 galaxies have weak $[\text{Fe X}]\lambda 6375$ emission in their spectra. This line was identified in high-ionization Seyfert galaxies by Grandi (1978) and is expected under a wide variety of photoionization conditions (Korista & Ferland 1989). Table 5 shows that it is apparently detected as a weak line in many narrow-line objects. The spectrum of NGC 5273, plotted in Figure 3, is a good example,

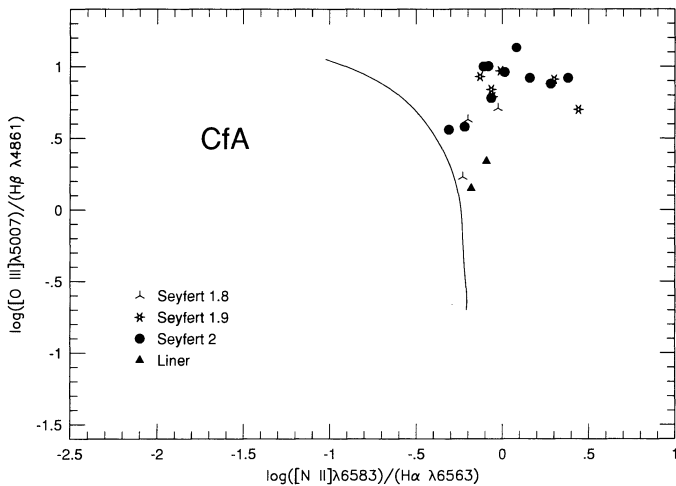


FIG. 6.—Reddening-corrected $[\text{O III}]\lambda 5007/\text{H}\beta$ vs. $[\text{N II}]\lambda 6583/\text{H}\alpha$ intensity ratios for galaxies from CfA sample. Solid curve divides AGNs from H II region-like objects (Veilleux & Osterbrock 1987).

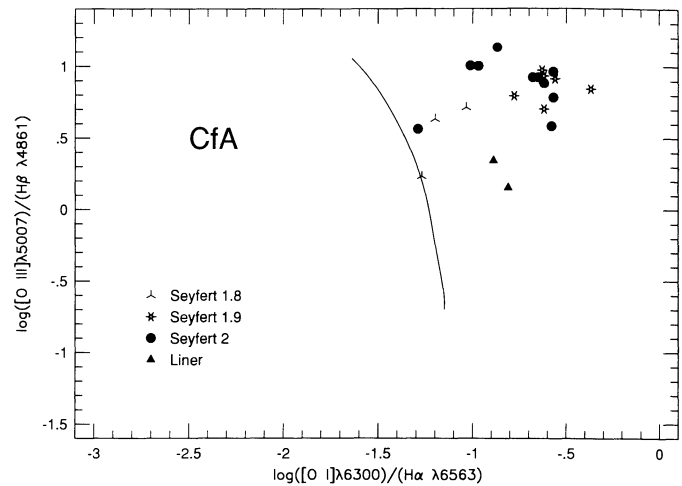


FIG. 8.—Reddening-corrected $[\text{O III}]\lambda 5007/\text{H}\beta$ vs. $[\text{O I}]\lambda 6300/\text{H}\alpha$ intensity ratios for galaxies from CfA sample. Solid curve as in Fig. 6.

where $[\text{Fe x}]$ shows as a weak, red wing of the $\lambda 6375$ blend, of which $[\text{O I}]\lambda 6364$ is the stronger component.

The errors in the measured weak, narrow emission-line fluxes are probably $\pm 20\%$, and the errors in the $[\text{Fe x}]\lambda 6375$ flux, calculated by subtraction, are correspondingly larger. However, in the cases in which the $[\text{Fe x}]\lambda 6375$ is largest, the measured blend shows a definite asymmetry to the red. Also, although we found many objects with calculable $[\text{Fe x}]\lambda 6375$ fluxes, only two objects (NGC 1144 and NGC 7682) in the sample yielded an apparently negative flux in this line, clearly the result of an observational error. Hence there are probably one or two objects in the sample with apparently measured $[\text{Fe x}]\lambda 6375$ which are also the result of observational error, but in many more cases the line appears to be present. As Korista & Ferland (1989) state, it can be understood to arise from photoionization by high-energy X-ray photons, although the presence of a high-temperature, coronal-like region heated by dissipation of mechanical energy is not ruled out.

Finally, the measured fluxes in the broad components of $\text{H}\beta$ and $\text{H}\alpha$, listed as $\text{H}\beta\text{b}$ and $\text{H}\alpha\text{b}$ respectively in Table 8, confirm

that in Seyfert 1.8 and 1.9 galaxies that $\text{H}\alpha\text{b}$ and $\text{H}\beta\text{b}$ ratios are generally higher than in typical Seyfert 1 and 1.5 objects (Osterbrock 1981; Goodrich 1989, 1990). As these authors state, this suggests, though in itself it does not prove, that in these objects strong extinction by dust is responsible for weakening considerably the broad-line spectrum.

7. MODEL AND EVOLUTION

The relative numbers of the various types of Seyfert galaxies may be used to estimate parameters in specific geometrical models or specific evolutionary pictures of Seyfert galaxies (Osterbrock & Shaw 1988). Here we take the results from the CfA sample as representative of Seyfert galaxies in general, here and now in the universe. The redshifts as tabulated by HB show that this means quantitatively out to redshift $z \lesssim 0.04$, with most of the weight of determination of the mean density of Seyfert 2 galaxies at considerably smaller values. The relative space densities, as stated in § 5, are Seyfert (1 + 1.5):Seyfert (1.8 + 1.9):Seyfert 2 = 0.22:0.25:0.53. The uncertainties in these ratios are largely the result of the limited number of objects in the sample, as stated by HB. This would give for the Seyfert 1.8 + 1.9 galaxies relative space density, 0.25 ± 0.09 . A more meaningful test is to compare two distributions by the χ^2 test, as outlined in § 3. The relative numbers of the various types of galaxies derived in the current paper are of course much better than any which simply ignore the Seyfert 1.8 and 1.9 classifications.

If we hypothesize that all Seyfert AGNs are more or less identical objects seen in different, random orientations, each built on the same “universal model” containing a luminous nucleus and broad-line region (BLR) surrounded by an optically thick obscuring torus or cylinder (Antonucci & Miller 1985; Lawrence 1987; Miller 1988; Krolik & Begelman 1988; Krolik & Lepp 1989), these numbers provide information on the projected area of the torus. In this picture the Seyfert 1 and 1.5 are objects seen nearly pole-on, within inclination θ between the axis of the torus and the line of sight $0 < \theta < \theta_1$, with $\theta_1 = \cos^{-1}(1 - 0.22) = 38^\circ$. Seyfert 2's, on the other hand, according to this model are objects seen nearly edge-on, so that none of the radiation emerges directly from the nucleus.

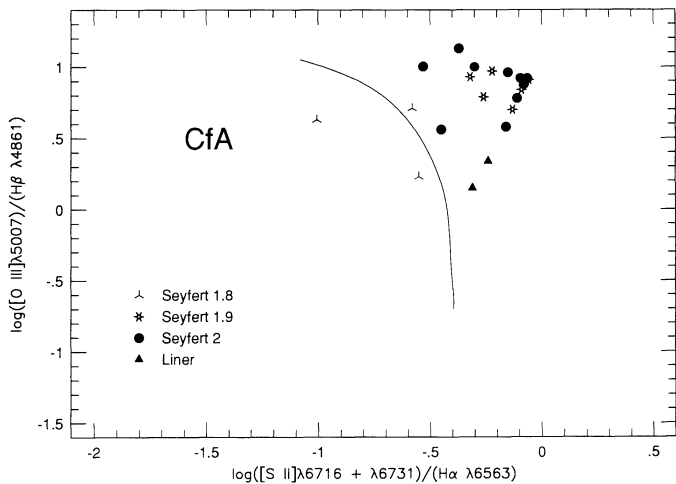


FIG. 7.—Reddening-corrected $[\text{O III}]\lambda 5007/\text{H}\beta$ vs. $[\text{S II}](\lambda 6717 + \lambda 6731)/\text{H}\alpha$ intensity ratios for galaxies from CfA sample. Solid curve as in Fig. 6.

For them $\theta_2 < \theta < \pi/2$, with $\theta_2 = \cos^{-1}(1 - 0.22 - 0.25) = 58^\circ$. The Seyfert 1.8 and 1.9 galaxies are objects which, in this picture, have nuclei partly but not completely obscured, corresponding either to intermediate optical depths, or more likely, distributions of clouds ranging between nearly complete blocking of the nucleus (at larger inclinations) to no blocking (at smaller inclinations) (Osterbrock & Shaw 1988). For such Seyfert 1.8 and 1.9 nuclei, $\theta_1 < \theta < \theta_2$. These angles can be translated, for instance, on the model of a point BLR at the centre of a torus with radius r and height h_1 above which there is no obscuration to $h_1/r = 2 \cot \theta_1 = 2.5$, and height h_2 below which the obscuration is total given by $h_2/r = 2 \cot \theta_2 = 1.3$. Seyferts which vary in time between Seyfert 1 or 1.5 and 1.9, such as NGC 4151, Mrk 530, and Mrk 993 would be exactly those with $\theta_1 < \theta < \theta_2$, or at least would be among them.

On this picture the opening angle of the ionization cone centered at the BLR would be $2\theta_1 = 76^\circ$. This value is somewhat larger than the mean value 50° which Pogge (1989) found for the opening angle in four Seyfert 2 galaxies, but in fair agreement with the values $65^\circ \pm 20^\circ$ found for the best studied Seyfert 2, NGC 1068, by Evans et al. (1991) from an HST image taken in [O III], or about 80° for the same object found by Bergeron, Petitjean, & Durret (1989), from long-slit spectroscopy in [Ne V] λ 3425.

In contrast, another, somewhat contradictory idea is that all AGNs evolve in time through a Seyfert 1 or 1.5 stage, then become Seyfert 1.8 or 1.9, then Seyfert 2, or perhaps alterna-

tively evolve the other way, or perhaps back and forth between these stages (Lawrence 1987). A somewhat more specific picture, in which some AGNs "begin" as Seyfert 1's, and follow the first path outlined above, while others "begin" as dusty Seyfert 2's, which evolve to Seyfert 1's, and then back to Seyfert 2's, has been put forward by one of us (Osterbrock 1993). On any evolutionary picture, the relative times a typical object spends in each stage are proportional to the fractions of objects observed in these stages, namely 0.22:0.25:0.53, or, more realistically, 0.2:0.3:0.5.

Obviously both the universal model and the strictly evolutionary picture are vast oversimplifications. But in confronting them with various different types of observational data, including the luminosity functions of the different types of Seyfert galaxies, we may hope to improve our understanding of these objects.

We are grateful for partial support of this research by the National Science Foundation under research grants AST 86-11457 and AST 91-23547. We are most grateful to John Huchra and Richard Burg for sending us their table of corrected radial velocities, distances, and absolute magnitudes, of the CfA AGNs, and for many most helpful discussions of this problem, their work on it, and our preliminary results. We also wish to thank Hien D. Tran for assistance in the data collection and reduction.

REFERENCES

- Antonucci, R. R. J., & Miller, J. S. 1985, *ApJ*, 297, 621
 Baldwin, J. E., Phillips, M. M., & Terlevich, R. 1981, *PASP*, 93, 5
 Bergeron, J., Petitjean, P., & Durret, F. 1989, *A&A*, 213, 61
 Bothun, G. D., Halpern, J. P., Lonsdale, C. P., Impey, C., & Schmitz, M. 1989, *ApJS*, 70, 271
 Cohen, R. D., & Antonucci, R. R. J. 1983, *ApJ*, 271, 564
 Dahari, O., & De Robertis, M. M. 1988, *ApJS*, 67, 249 (DD)
 Edelson, R. 1987, *ApJ*, 313, 651
 Evans, I. N., Ford, H. C., Kinney, A. L., Antonucci, R. R. J., Armus, L., & Cagonoff, S. 1991, *ApJ*, 368, L27
 Felten, J. 1977, *AJ*, 82, 861
 Filippenko, A. V. 1985, *ApJ*, 289, 475
 Filippenko, A. V., & Sargent, W. L. W. 1989, *ApJ*, 342, L11
 Goodrich, R. W. 1989, *ApJ*, 340, 190
 ———. 1990, *ApJ*, 355, 88
 Grandi, S. A. 1978, *ApJ*, 221, 501
 Huchra, J., & Burg, R. 1992, *ApJ*, 393, 90 (HB)
 Huchra, J., Davis, M., Latham, D., & Tonry, J. 1983, *ApJS*, 52, 89
 Huchra, J., & Sargent, W. L. W. 1973, *ApJ*, 186, 433
 Huchra, J., Wyatt, W., & Davis, M. 1982, *AJ*, 87, 1628
 Korista, K. T., & Ferland, G. J. 1989, *ApJ*, 343, 678
 Krolik, J. H., & Begelman, M. C. 1988, *ApJ*, 329, 702
 Krolik, J. H., & Lepp, S. 1989, *ApJ*, 347, 1989
 Lawrence, A. 1987, *PASP*, 99, 309
 Lipovetsky, V. A., Markarian, B. E., & Stepanian, J. A. 1987, in *IAU Symp.* 121, *Observational Evidence of Activity in Galaxies*, ed. E. Ye. Khachikian, K. J. Fricke, & J. Melnick (Dordrecht: Reidel), 17
 Miller, J. S. 1988, in *Active Galactic Nuclei*, ed. H. R. Miller & P. J. Wiita (Berlin: Springer-Verlag), 239
 Miller, J. S., Robinson, L. B., & Goodrich, R. W. 1988, *Instrumentation for Ground-Based Optical Astronomy*, ed. L. B. Robinson (New York: Springer-Verlag), 157
 Osterbrock, D. E. 1981, *ApJ*, 249, 462
 ———. 1987, in *IAU Symp.* 121, *Observational Evidence of Activity in Galaxies*, ed. E. Ye. Khachikian, K. J. Fricke, & J. Melnick (Dordrecht: Reidel), 109
 ———. 1993, *ApJ*, 404, 551
 Osterbrock, D. E., & Shaw, R. A. 1988, *ApJ*, 327, 89
 Penston, M. V., & Perez, E. 1984, *MNRAS*, 211, 33P
 Pogge, R. W. 1989, *ApJ*, 345, 730
 Salzer, J. J. 1989, *ApJ*, 347, 152
 Schmidt, M. 1968, *ApJ*, 151, 393
 Tohline, J. E., & Osterbrock, D. E. 1976, *ApJ*, 210, L117
 Tran, H. D., Osterbrock, D. E., & Martel, A. 1992, *AJ*, 104, 2072
 Veilleux, S., & Osterbrock, D. E. 1987, *ApJS*, 63, 295
 Véron-Cetty, M. P., & Véron, P. 1986, *A&AS*, 65, 241
 Wasilewski, A. 1983, *ApJ*, 272, 68